



Towards small target recognition with photonics-based high resolution radar range profiles

JINHU LI, FANGZHENG ZHANG,*  YU XIANG, AND SHILONG PAN 

Key Laboratory of Radar Imaging and Microwave Photonics, Ministry of Education, Nanjing University of Aeronautics and Astronautics, Nanjing 210016, China

*zhangfangzheng@nuaa.edu.cn

Abstract: Photonics-based radar expands the bandwidth of traditional radars and enhances the radar range resolution. This makes it possible to recognize small-size targets using the high resolution range profiles (HRRPs) acquired by a photonics-based broadband radar. In this paper, we investigate the performance of small target recognition using HRRPs of a photonics-based radar with a bandwidth of 8 GHz (28-36 GHz), which is built based on photonic frequency multiplication and frequency mixing. A convolutional neural network (CNN) is used to extract features of the HRRPs and classify the targets. In the experiment, recognition of four types of small-size targets is demonstrated with an accuracy of 97.16%, which is higher than target recognition using a 77-GHz electronic radar by 31.57% (2-GHz bandwidth) and 8.37% (4 GHz-bandwidth), respectively. Besides the accuracy, target recognition with photonics-based radar HRRPs is proved to have good generalization capability and stable performance. Therefore, photonics-based radar provides an efficient solution to small target recognition with one-dimension HRRPs, which is expected to find import applications in air defense, security check, and intelligent transportation.

© 2021 Optical Society of America under the terms of the [OSA Open Access Publishing Agreement](#)

1. Introduction

Radar target recognition has important applications in military and civil fields [1]. Typically, radar target recognition can be realized based on one-dimensional (1D) high-resolution range profiles (HRRP) or two-dimensional (2D) high-resolution images of a target [2,3]. Although the 2D high-resolution images obtained by a synthetic aperture radar (SAR) have been widely investigated for radar target recognition, the hardware requirements and computational complexity for constructing such high-resolution SAR images are very high. Compared with image-based radar target recognition, the HRRP-based target recognition has the advantages of easy acquisition, stable resolution, and small amount of calculation. Therefore, HRRP-based radar target recognition has attracted lots of attention and has been applied in military applications such as air target recognition. However, since the range resolution of traditional radars is limited by the bandwidth of electrical devices and subsystems, HRRP-based radar target recognition is usually used to detect large size targets such as airplanes and missiles. As the modern radar faces increasingly complex environment, it is highly desirable to recognize small targets, such as small drones, using the radar HRRPs. In recent years, photonics-based radar has been intensively investigated [4–9], which greatly expands the radar bandwidth by photonic generation and processing of broadband radar signals. Previously, photonics-based synthetic aperture radar, phased array radar, and multiple-input and multiple-output (MIMO) radar have been successfully demonstrated [10–16], in which the range resolution reaches as high as centimeter level [17]. The ultra-high range resolution of photonics-based radars makes it possible for small target recognition with HRRPs. It is expected that target recognition with photonics-based radar HRRP may play a new and important role in applications such as security check and automatic driving. In [18], Wan *et al.* demonstrated the HRRP-based target recognition using a photonic analog-to-digital converter

(PADC) to improve the sampling rate of the radar receiver. In their work, by transmitting radar signals with a bandwidth of 2 GHz, high-accuracy recognition of artificially constructed small-size objects was achieved.

In this paper, we investigate the performance of small target recognition based on the HRRPs of a photonics-based broadband radar. Different from the work in [18] where the operation bandwidth is limited by the electric radar transmitter, the photonics-based radar we used has a much larger bandwidth of 8 GHz (28-36 GHz), which is enabled by broadband microwave photonic signal generation in the transmitter and broadband microwave photonic signal processing in the receiver. What's more, the small-size targets in our experiment are articles for daily use, imitating the security check scenario. In our method, the feature extraction from the HRRPs and target classification are implemented by a convolutional neural network. The performance of target recognition using the photonics-based radar is also compared with that by using an electronic 77-GHz radar with a bandwidth of 2 GHz and 4 GHz, respectively.

2. Principle

Radar HRRP is the projection of scatterers of a target to the radar line of sight (LOS). It is a one-dimensional signature of an object that can be used for target recognition. Usually, the radar range resolution is smaller than the size of the target, and hence the target can be divided into multiple range cells along the radar LOS, as shown in Fig. 1, in which the target is a pistol and the conditions of low-range-resolution detection and high-range-resolution detection are both included. For detection using a low-range-resolution radar, as shown on the left side of Fig. 1, the range profile in each range cell is dependent on the coherent synthesis of the echoes of all the scatterers within the same range cell. As a result, the range profile may not reflect the actual distribution of the scatterers of the target, which influences the recognition accuracy. On the other hand, if the target is detected by a high-range-resolution radar, the target would be covered by more range cells, and more peaks and fluctuations revealing the scatterer distributions are observed in the range profile, as shown on the right side of Fig. 1. In this case, a more accurate relationship between the range profile and the detailed structure information of the target can be established. From this perspective, a high range resolution radar is highly desired to achieve a high target recognition accuracy. To this end, we apply a photonics-based radar that has an operation bandwidth of 8 GHz, corresponding to a range resolution as high as 1.875 cm, which is expected to permit the recognition of small targets with very high accuracy.

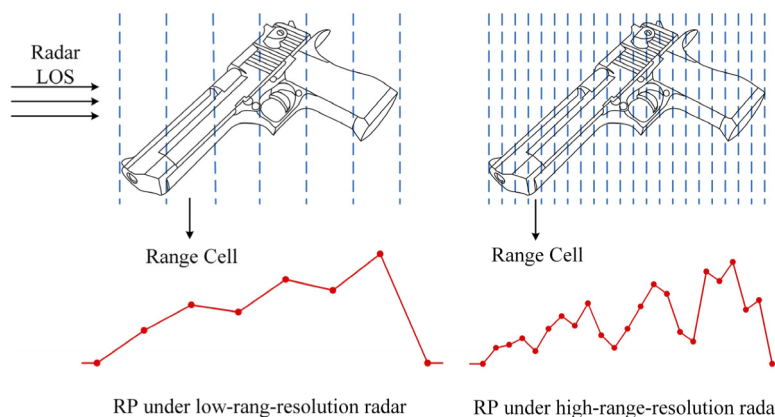


Fig. 1. Range profiles of a pistol acquired by a low-resolution radar and a high-resolution radar.

Figure 2(a) shows the photonics-based radar prototype that is build based on microwave photonic frequency multiplication in the transmitter and microwave photonic frequency mixing in the receiver. Figure 2(b) is the schematic diagram of the photonics-based radar. A voltage-controlled oscillator (VCO) is used to generate a linearly frequency-modulated (LFM) signal having a bandwidth of 2 GHz (7–9 GHz). After the LFM signal passes through an electrical 90° hybrid coupler, the two output signals are sent to the two RF ports of a dual-parallel Mach-Zehnder modulator (DPMZM) to modulate a continuous wave light from a laser diode (LD). By properly adjusting the bias voltage, the DPMZM works in frequency quadrupling mode [6]. Then, the generated optical signal is equally divided into two branches by an optical coupler (OC). In the upper branch, a frequency quadrupled signal with a bandwidth of 8 GHz (28–36 GHz) is generated after optical-to-electrical conversion at a photodetector (PD1). This signal is amplified by an electrical amplifier (EA1) before emitted to the detection area. The radar echo signal is amplified by another amplifier (EA2) before applied to a Mach-Zehnder modulator (MZM) to modulate the optical signal from the lower branch of the OC. The output optical signal is amplified by an erbium-doped optical fiber amplifier (EDFA) and then enters PD2 to implement photonic frequency mixing, which completes the de-chirp processing [12]. An electrical low-pass filter (ELPF) is used to remove the high-frequency interference, and de-chirped signal is sampled by an analog-to-digital converter (ADC). Then, fast Fourier transformation (FFT) is performed on the digital signals to get the HRRPs of the target [6].

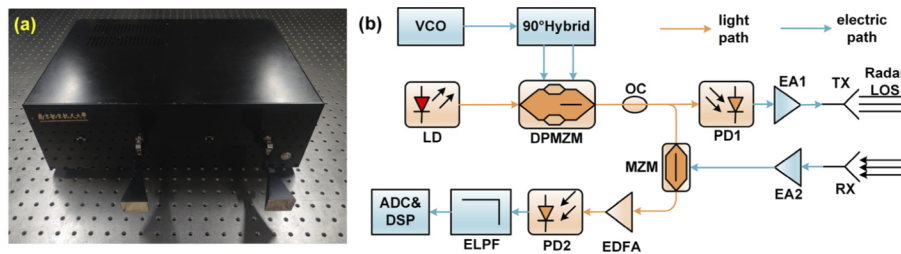


Fig. 2. (a) Picture of photonics-based radar prototype, and (b) schematic diagram of the photonics-based radar.

Based on the obtained HRRPs, a 1D CNN is established to perform feature extraction and target classification. Compared with the traditional target recognition by template matching and other machine learning based classification models such as the support vector machine (SVM), the CNN-based target recognition has been proved to be more powerful to obtain the hidden features from the HRRPs and have strong generalization capability [18,19]. Figure 3 shows the

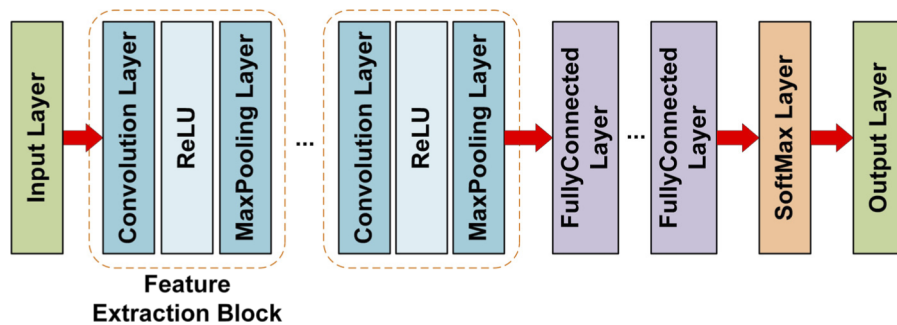


Fig. 3. Structure of the 1D convolutional neural network used for feature extraction and classification.

structure of the CNN we used, which is composed of an input layer, several feature extraction blocks, several fully connected layers, a softmax layer, and an output layer. The input layer inputs the preprocessed HRRPs into the CNN. The feature extraction block consists of a 1D convolution layer used for extracting the local feature of the HRRPs, a rectified linear unit (ReLU) as the nonlinear activation function, and a max pooling layer that implements feature selection and dimensionality reduction through down sampling. The fully connected layer arranges the extracted features into one-dimensional vectors by nonlinear mapping. Finally, the softmax layer works as the classifier, and output layer gives the classification result.

3. Experiments

The targets to be recognized are four small-size objects: a pistol (target A), a scissors (target B), a hammer (target C), and a kitchen knife (target D). These targets are chosen to imitate the scenario of security check, and their shapes and sizes are shown in Figs. 4(a), 4(c), 4(e), and 4(g), respectively. In the experiment, to enhance the scattering intensity, all the targets are wrapped with aluminum foil. To compare the performance of target recognition with different radar bandwidths, a commercial radar produced by Texas Instruments (TI: AWR1243 BOOST) is also applied, which has a maximum bandwidth of 4 GHz around 77 GHz. Here, the TI radar is a narrow band radar since its relative bandwidth is smaller than 10%. The repetition rate of the TI radar and photonics-based radar is 1.5 kHz and 1.25 kHz, respectively, and the pulse duty cycle is 37.5% and 45%, respectively. Besides, the emitting power is 12 dBm and 13 dBm for the TI radar and photonics-based radar, respectively. The detailed information of the photonics-based radar and its comparison with electronic radars are provided in [6,11]. In the experiment, the antenna of the two radars have a depression angle of about 13 degree towards the target, and the distance between radar and target is about 0.4 m.

In the experiment, the TI radar is set to work with a bandwidth of 2 GHz (77-79 GHz) and 4 GHz (77-81 GHz), respectively, which are denoted by TI radar (2 GHz) and TI radar (4 GHz) throughout the rest of this paper. The range resolution of TI radar (2 GHz) and TI radar (4 GHz) is 7.5 cm and 3.75 cm, respectively. Along the radar LOS shown in Figs. 4(a), 4(c), 4(e), and 4(g), the HRRPs of the four targets obtained by the TI radar and the photonics-based radar are shown in Figs. 4(b), 4(d), 4(f), and 4(h), respectively. It is obvious that, more peaks and details are observed in the photonics-based radar HRRPs for all the targets, which indicates the photonics-based radar HRRPs are more informative compared with the HRRPs obtained by the TI radar.

To make sure the target recognition is reliable as the observation angle changes, multiple HRRPs are collected by rotating the target. Specifically, 360 HRRPs of each target are obtained by rotating the target by 1 degree at a time. There are 1440 HRRPs sampled by the TI radar (2 GHz), the TI radar (4 GHz) and the photonics-based radar, respectively. Among all the samples, 80% of the HRRPs of each target are randomly chosen to compose the training dataset, and the other 20% are used as the testing dataset. Before sent to the CNN, all the HRRPs are normalized and interpolated to a length of 128. The CNN is optimized to have three convolution layers, three max pooling layers, and two fully connected layers. The detailed parameters of the CNN are shown in Table 1. Training and testing the CNN is implemented using the Deep Learning Toolbox in MATLAB. In the training process, the learning rate is 0.01 and the random gradient descent algorithm is applied to update the network parameters. The CNN is trained and tested using a computer with an AMD R7-4800H CPU (8-core) and an NVIDIA Geforce-RTX-2060 GPU.

Figure 5(a) shows the classification accuracy during training and testing the CNN in different epochs considering all the three radar detection conditions. As shown in Fig. 5(a), the testing accuracy tends to be convergent when the number of epochs reaches 200 for all the three radar detection conditions. To avoid overfitting, the training was early stopped as the epoch number

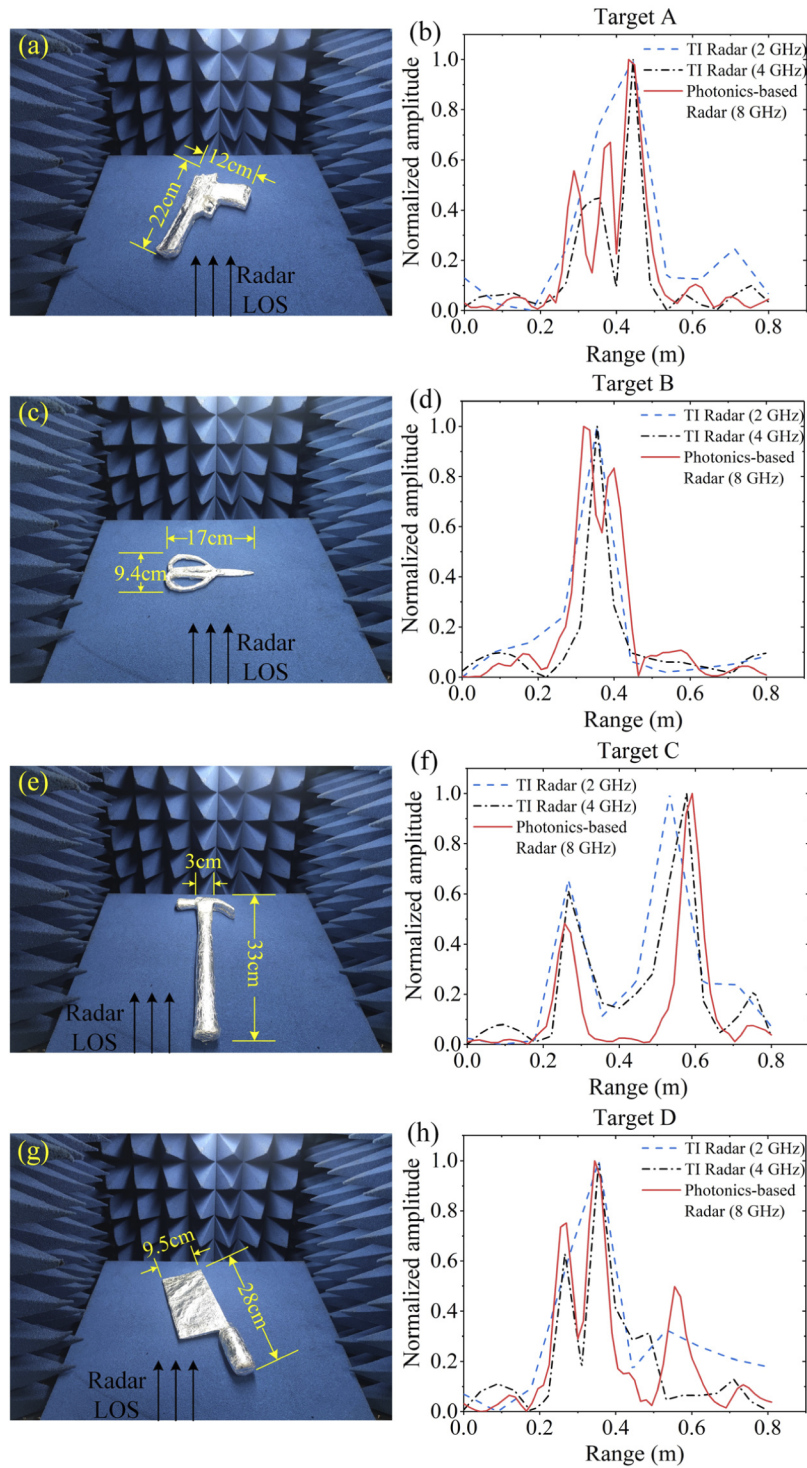


Fig. 4. (a), (c), (e), (g) Pictures of target A, target B, target C, and target D. (b), (d), (f), (h) HRRPs of the four targets.

Table 1. Parameters of the optimized 1D CNN

Layer name	Feature Size	Filter size	Stride	Number of channels
Input Layer	1×128	/	/	/
Convolution Layer-1	1×126	1×3	1	64
Max Pooling Layer-1	1×42	1×3	3	64
Convolution Layer -2	1×40	1×3	1	128
Max Pooling Layer-2	1×20	1×2	2	128
Convolution Layer -3	1×16	1×5	1	256
Max Pooling Layer-3	1×8	1×2	2	256
Fully Connected Layer-1	1×2048	/	/	/
Fully Connected Layer-2	1×4	/	/	/

researches 250. The whole training processing takes about 2 minutes. The final recognition accuracy (the testing accuracy) is found to be 65.59%, 88.79% and 97.16%, by using the TI radar (2 GHz), the TI radar (4 GHz), and the photonics-based radar, respectively, as shown in Fig. 5(b). Apparently, the photonics-based radar achieves much higher accuracy for target recognition. It is also found that, the testing accuracy for TI radar (2 GHz) and TI radar (4 GHz) is 16.41% and 9.24% lower than the corresponding training accuracy, respectively, while the testing accuracy for the photonics-based radar is only 2.81% lower than the training accuracy. This indicates the CNN trained with the HRRPs of the photonics-based radar has much stronger generalization capability. To intuitively show the advantage of target classification with the photonics-based radar, the features extracted at the output of the second fully connected layer are visualized by t-SNE algorithm [20], with the results in Fig. 6. For TI radar (2 GHz), the targets of different types are mixed and they cover a large area in the feature space, corresponding to a low classification accuracy. For TI radar (4 GHz), different types of targets are separated better than those for TI radar (2 GHz), but there are still obvious overlaps, especially between target C and target D. For photonics-based radar, the targets of different types are converged to separated areas with very few exceptions. The discriminative feature space of the photonics-based radar corresponds well with the high recognition accuracy.

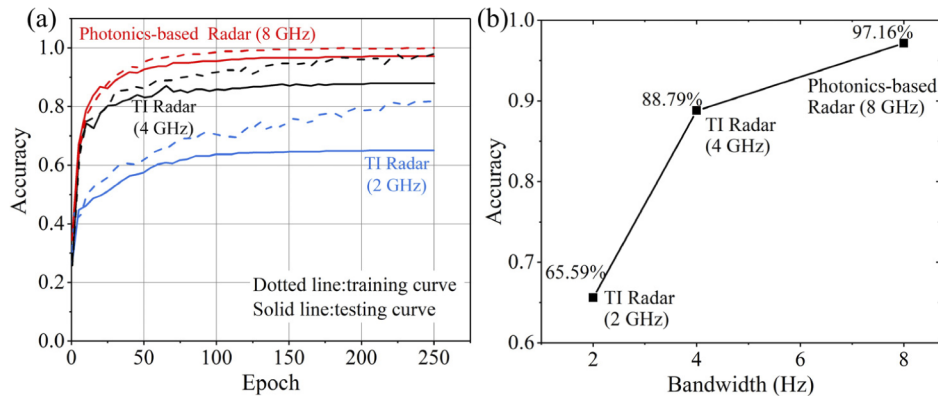


Fig. 5. (a) The training and testing accuracy curves considering all the three detection conditions, and (b) the relationship between the bandwidth and the final recognition accuracy.

In the previous analysis, the target recognition accuracy is the average accuracy considering all the four types of targets. Figure 7 shows the confusion matrices revealing the recognition accuracy of each type of target when using different radars. By comparing the three confusion

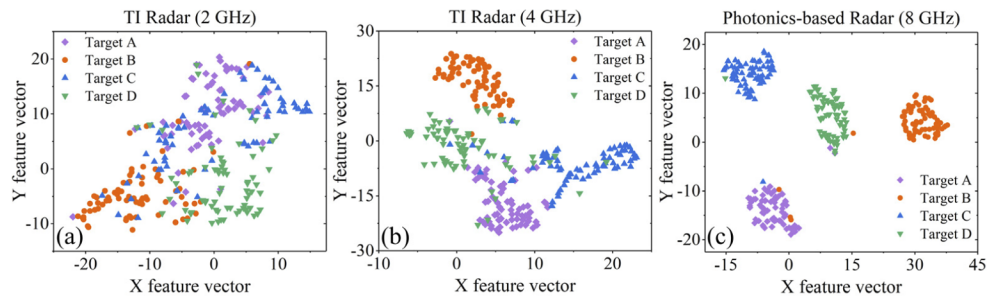


Fig. 6. t-SNE feature visualizations for (a) TI Radar (2 GHz), (b) TI Radar (4 GHz), and (c) Photonics-based Radar.

matrices in Fig. 7, it is obvious that the recognition of each target with photonics-based radar has the highest accuracy, which confirms the advantage of photonics-based broadband radar again. The results in Fig. 7 also show that, when using a low-resolution radar, the recognition accuracy of different targets may vary significantly, e.g., the recognition accuracy of target C is remarkably lower than the other targets by over 15% for the case of TI radar (2 GHz). While, as the radar bandwidth increases, i.e., the resolution of the HRRPs is improved, the accuracy difference between different targets is reduced. Specially, for the photonics-based broadband radar, the variation of recognition accuracies of different targets is less than 4%. Therefore, the photonics-based radar has much more stable recognition capability for all the targets. This is attributed to its ultra-high range resolution that makes the HRRPs of different targets have easily distinguishable features.

	(a) TI Radar (2 GHz)				(b) TI Radar (4 GHz)				(c) Photonics-based Radar (8 GHz)			
True category	TargetA	TargetB	TargetC	TargetD	TargetA	TargetB	TargetC	TargetD	TargetA	TargetB	TargetC	TargetD
TargetA	68.9%	8.9%	17.8%	4.4%	88.9%		1.8%	9.3%	98.1%	1.2%		0.7%
TargetB	14.6%	68.3%	12.2%	4.9%	2.8%	94.4%		2.8%	2.8%	94.4%	2.8%	
TargetC	18.9%	9.4%	50.9%	20.8%	6.4%	2.1%	87.2%	4.3%		0.6%	98.0%	1.4%
TargetD	14.3%	16.3%	4.1%	65.3%	9.4%	7.5%	3.8%	79.3%	0.8%		2.9%	96.3%
Forecast category	TargetA	TargetB	TargetC	TargetD	TargetA	TargetB	TargetC	TargetD	TargetA	TargetB	TargetC	TargetD

Fig. 7. Confusion matrix of (a) TI Radar (2 GHz), (b) TI Radar (4 GHz), (c) Photonics-based Radar (8 GHz).

4. Discussion and conclusion

In our investigation, the photonics-based radar and TI radar work in different frequency bands. While, this does not affect the reliability of the comparison results, because the range resolution is mainly determined by the radar bandwidth. In practical applications, the HRRP usually contains complex information about the detection environment. To cope with this problem, a proper segmentation technique should be applied to extract the specific section of the HRRP corresponding to the desired target. In addition, more HRRPs of targets with different shapes and sizes are preferred to train the CNN, with can help to recognize more targets with different features. Furthermore, normalization of the HRRPs is recommend to recognize targets with different scattering intensities, and other preprocessing techniques such as power multiplication operation can be applied to further improve the recognition accuracy [21].

In conclusion, we have investigated the performance of small target recognition with HRRPs of a photonics-based radar, in which a CNN is applied for feature extraction and target recognition. The experimental results show that it is possible to recognize small targets by the HRRPs of a photonics-based broadband radar, thanks to its ultra-high range resolution. In the experiment, the target recognition accuracy of the photonics-based radar (8-GHz bandwidth) is higher than traditional radar by 31.57% (2-GHz bandwidth) and 8.37% (4 GHz-bandwidth), respectively. In addition to the high recognition accuracy, the photonics-based radar is also proved to have stable recognition performance for different types of targets.

Funding. National Natural Science Foundation of China (61871214, 11804159); Natural Science Foundation of Jiangsu Province (BK20180066).

Disclosures. The authors declare no conflicts of interest.

Data availability. Data underlying the results presented in this paper are not publicly available at this time but may be obtained from the authors upon reasonable request.

References

1. J. Gomes, J. Brancalion, and D. Fernandes, "Automatic Target Recognition in Synthetic Aperture Radar image using multiresolution analysis and classifiers combination," *2008 IEEE Radar Conference* (2008), pp. 1–5.
2. R. Williams, J. Westerkamp, D. Gross, A. Palomion, and T. Fister, "Automatic target recognition of time critical moving targets using 1D high range resolution (HRR) radar," *1999 IEEE Radar Conference* (1999), pp. 54–59.
3. B. Ding, G. Wen, F. Ye, X. Huang, and X. Yang, "Feature extraction based on 2D compressive sensing for SAR automatic target recognition," *2017 11th European Conference on Antennas and Propagation (EUCAP)* (2017), pp. 1219–1223.
4. P. Ghelfi, F. Laghezza, F. Scotti, G. Serafino, A. Capria, S. Pinna, D. Onori, C. Porzi, M. Scaffardi, A. Malacarne, V. Vercesi, E. Lazzeri, F. Berizzi, and A. Bogoni, "A fully photonics-based coherent radar system," *Nature* **507**(7492), 341–345 (2014).
5. W. Zou, H. Zhang, X. Long, S. Zhang, Y. Cui, and J. Chen, "All optical central-frequency-programmable and bandwidth tailorable radar," *Sci. Rep.* **6**, 19786 (2016).
6. F. Zhang, Q. Guo, and S. Pan, "Photonics-based real-time ultra-high-range-resolution radar with broadband signal generation and processing," *Sci. Rep.* **7**(1), 13848 (2017).
7. R. Li, W. Li, M. Ding, Z. Wen, Y. Li, L. Zhou, S. Yu, T. Xing, B. Gao, Y. Luan, Y. Zhu, P. Guo, Y. Tian, and X. Liang, "Demonstration of a microwave photonic synthetic aperture radar based on photonic-assisted signal generation and stretch processing," *Opt. Express* **25**(13), 14334–14340 (2017).
8. J. Shi, F. Zhang, D. Ben, and S. Pan, "Simultaneous Radar Detection and Frequency Measurement by Broadband Microwave Photonic Processing," *J. Lightwave Technol.* **38**(8), 2171–2179 (2020).
9. S. Peng, S. Li, X. Xue, X. Xiao, D. Wu, X. Zheng, and B. Zhou, "High-resolution W-band ISAR imaging system utilizing a logic-operation-based photonic digital-to-analog converter," *Opt. Express* **26**(2), 1978–1987 (2018).
10. J. Dong, F. Zhang, Z. Jiao, Q. Sun, and W. Li, "Microwave photonic radar with a fiber-distributed antenna array for three-dimensional imaging," *Opt. Express* **28**(13), 19113–19125 (2020).
11. F. Zhang, Q. Guo, Z. Wang, P. Zhou, G. Zhang, J. Sun, and S. Pan, "Photonics-based broadband radar for high-resolution and real-time inverse synthetic aperture imaging," *Opt. Express* **25**(14), 16274–16281 (2017).
12. B. Gao, F. Zhang, E. Zhao, D. Zhang, and S. Pan, "High-resolution phased array radar imaging by photonics-based broadband digital beamforming," *Opt. Express* **27**(9), 13194–13203 (2019).
13. G. Sun, F. Zhang, B. Gao, Y. Zhou, Y. Xiang, and S. Pan, "Photonics-based 3D radar imaging with CNN-assisted fast and noise-resistant image construction," *Opt. Express* **29**(13), 19352 (2021).
14. F. Zhang, B. Gao, and S. Pan, "Photonics-based MIMO radar with high-resolution and fast detection capability," *Opt. Express* **26**(13), 17529–17540 (2018).
15. B. Gao, F. Zhang, G. Sun, Y. Xiang, and S. Pan, "Microwave Photonic MIMO Radar for High-resolution Imaging," *J. Lightwave Technol.*, to appear, doi: 10.1109/JLT.2021.3070591. (2021).
16. S. Pan, X. Ye, Y. Zhang, and F. Zhang, "Microwave photonic array radars," *IEEE J. Microw.* **1**(1), 176–190 (2021).
17. Y. Yao F. Y. Zhang and X. Zhang, D. Ye, S. Zhu, and Pan, "Demonstration of ultra-high-resolution photonics-based Ka-band inverse synthetic aperture radar imaging," OFC 2018, paper. Th3G.5
18. J. Wan, S. Xu, and W. Zou, "High-accuracy automatic target recognition scheme based on a photonic analog-to-digital converter and a convolutional neural network," *Opt. Lett.* **45**(24), 6855–6858 (2020).
19. J. Wan, B. Chen, Y. Yuan, H. Liu, and L. Jin, "Radar HRRP Recognition using Attentional CNN with Multi-resolution Spectrograms," 2019 International Radar Conference (RADAR) (2019), pp. 1–4.
20. M. Pan, J. Jiang, Q. Kong, J. Shi, Q. Sheng, and T. Zhou, "Radar HRRP Target Recognition Based on t-SNE Segmentation and Discriminant Deep Belief Network," *IEEE Geosci. Remote Sensing Lett.* **14**(9), 1609–1613 (2017).
21. Y. Shi and X. Zhang, "A Gabor atom network for signal classification with application in radar target recognition," *IEEE Trans. Signal Process.* **49**(12), 2994–3004 (2001).